

Electronic Supplementary Information

Synergistic Effect of Au and Rh on SrTiO₃ in Significantly Promoting Visible-Light-Driven Syngas Production from CO₂ and H₂O

Dewang Li,^{ab#} Shuxin Ouyang,^{abc#*} Hua Xu,^{abc} Da Lu,^{ab} Ming Zhao,^{ab} Xueliang Zhang,^{ab} Jinhua Ye^{abcd*}

^a *TU-NIMS Joint Research Center, School of Materials Science and Engineering, Tianjin University, Tianjin 300072, P.R. China.*

^b *Collaborative Innovation Center of Chemical Science and Engineering (Tianjin), Tianjin 30072, P. R. China.*

^c *Tianjin Key Laboratory of Composite and Functional Materials, and Key Lab of Advanced Ceramics and Machining Technology, Ministry of Education, Tianjin 300072, PR China.*

^d *International Center for Materials Nanoarchitectonics (WPI-MANA) and Environmental Remediation Materials Unit, National Institute for Materials Science (NIMS), Japan.*

* Author to whom correspondence should be addressed.

Electronic mail: oyxs@tju.edu.cn; jinhua.ye@nims.go.jp

These authors contributed to this work equally.

Experimental Section

Photocatalyst Preparation. The SrTiO₃ adopted in this study is a commercial-available sample (Aldrich, 99.5%). The AuCl₃·HCl·4H₂O, Na₃RhCl₆ and RhCl₃ were prepared to be precursor solutions with certain concentration. For grafting Rh cocatalyst by impregnation method, a certain volume of Na₃RhCl₆ solution was added into the mixture of 50 mL deionized water and 0.5 g dispersed SrTiO₃ powder according to loading amount, and then the suspension was vaporated under stirring until complete drying. The resulting powder was calcinated at 500 °C for 2 h to form

Rh₂O₃ attached on SrTiO₃, followed by heating at 500 °C under H₂/Ar mixture (v/v=1:9, flow rate 20 mL/min) for 2 h to reduce metal oxides into metal species. For grafting Rh cocatalyst by photodeposition, a certain volume of RhCl₃ solution according to 0.5wt% loading amount was added into the mixture of 220 mL deionized water, 50 mL methanol, 2 mL HCl solution (36.5 wt%) and 0.5 g dispersed SrTiO₃ powder. The vessel containing above substance was then evacuated until no air was left, followed by UV irradiation for 1 h to load Rh particles on SrTiO₃.

To load Au, 0.2 g sample of the Rh@STO or the STO for reference was dispersed in methanol solution and then ultrasonicated. The precursor solution of Au with the volume corresponding to certain loading amount was added in the suspension and then photo-deposition under visible-light irradiation for 1 h was carried out. After the irradiation, the mixture was centrifuged and washed for 4 times to remove the residual methanol, followed by dried at 80°C. Finally, the Ru-Au@STO or Au@STO was dried at 80°C in air.

To optimize the loading amounts of Au or Rh nanoparticles on SrTiO₃ for best productivity, the amount of Au or Rh were varied to the value of 0.25wt%, 1.0wt% and 1.5wt% respectively when the amount of the other metal remained at 0.5wt%. The different loading amounts were realized by means of adding precursors corresponding to the desired amounts in loading procedure. The samples are labeled as xRh-0.5Au@ STO and 0.5Rh-yAu@STO, respectively.

Characterizations. The Transmission electron microscopy (TEM) and high resolution TEM images were taken by a field emission transmission electron microscope (2100F, JEOL Co., Japan) operated at 200 kV for morphology and phase observation. Diffuse reflection spectra ranged from 300 to 800 nm was recorded by UV-vis spectrometer (UV-2700, Shimadzu) and then converted into absorption spectra via Kubelka–Munk transformation. Photoluminescence (PL) spectra were recorded on a fluorescence spectrophotometer (Fluorolog-3, HORIBA Scientific, America).

Photoreduction Evaluation. A 75 mg sample was spread onto an air-permeable

quartz fiber filter. About 3 mL deionized water was injected into the bottom of the reactor. After 30 min evacuation, the air in the system was removed completely which could be confirmed by gas chromatograph, and then CO₂ as reactant was slowly injected into reaction system until the pressure in system increased to about 70 kPa. After that, the gas circulation pump and the 300-W Xe lamp with a filter L42 that only allows light with wavelength $\lambda > 400$ nm to pass through were turned on. At certain time interval, the H₂, CO and CH₄ were detected by injecting 0.5 mL gas mixture into gas chromatograph (GC-2014C for H₂ and O₂ measurement, GC-2014 for CO and CH₄ measurement, Shimadzu, Japan).

Photocurrent Measurement. The photoanode thin films of Au@STO and Rh-Au@STO were prepared by a spin-coating method. In a typical procedure, 5 mg of as-prepared powder sample was dispersed in 3 mL of ethanol by ultrasonic treatment for 30 min. The obtained suspension was spin-coated layer by layer with a spin setting of 200 rpm for 10 s and then 600 rpm for 30 s. Finally, the thin film was heated with a temperature ramp of 1°C/min and kept at 350°C for 2 h. The photocurrent measurements were carried out in a three-electrode configuration system (Au@STO or Rh-Au@STO anode as working electrode, Pt foil as counter-electrode, and

Photocatalyst / using mass (g)	Illumination / reaction system	CO and H ₂ Evolution Rates ($\mu\text{mol}/(\text{h}\cdot\text{g})$)	Reference
Re complex / 1-2 μmol	450-W Xe lamp with a 300 nm cut-off filter / 0.1 mL of triethylamine (TEA) as sacrificial reducing agent	CO: 0.545 H ₂ : 0.125	<i>J. Am. Chem. Soc.</i> , 2011 , 133, 13445-13454
Ag(1 wt %)-BaLa ₄ Ti ₄ O ₁₅ / 0.3 g	400-W Hg lamp / 360 mL water, CO ₂ flow system (15 mL/min)	CO: 14.3 H ₂ : 33.3	<i>J. Am. Chem. Soc.</i> , 2011 , 133, 20863-20868
TiO ₂ (325 mesh) / 0.05 g	Rayonet photoreactor (350 nm) / CO ₂ -purged 5 mL water with 0.5 M 2-propanol	CO: ~4.8 H ₂ : ~2.9	<i>Res. Chem. Intermed.</i> , 2007 , 33, 631-644
1-dodecanethiol(1.3 mol%)-modified CdS / 0.01 g	500-W Hg lamp with a 300 nm cut-off filter / CO ₂ saturated dichloromethane solution containing 1.0 mol/L 2-propanol	CO: ~7.1 H ₂ : ~20.0	<i>J. Photochem. Photobiol. A-Chem.</i> , 1998 , 113, 93-97
Ru-Au coloaded SrTiO ₃ / 0.075 g (Ru was loaded by impregnation process)	300-W Xe lamp with L42 cut-off filter ($\lambda > 400$ nm) / 3 mL H ₂ O and 70 kPa CO ₂	CO: 66.8 H ₂ : 50.5	This study
Ru(PD)-Au coloaded SrTiO ₃ / 0.075 g (Ru was loaded by photodeposition process)	300-W Xe lamp with L42 cut-off filter ($\lambda > 400$ nm) / 3 mL H ₂ O and 70 kPa CO ₂	CO: 369.2 H ₂ : 69.4	

Ag/AgCl electrode as reference electrode) by using a CHI electrochemical station (ALS/CH model 650A) with 0.1 M Na₂SO₄ aqueous solution as electrolyte and 0.6 V bias voltage. A 500 W Xe arc lamp equipped with a L42 cutoff filter ($\lambda > 400$ nm) was used as light source.

Table S1. Photoactivity comparison of previous studies on syngas photosynthesis and this study.

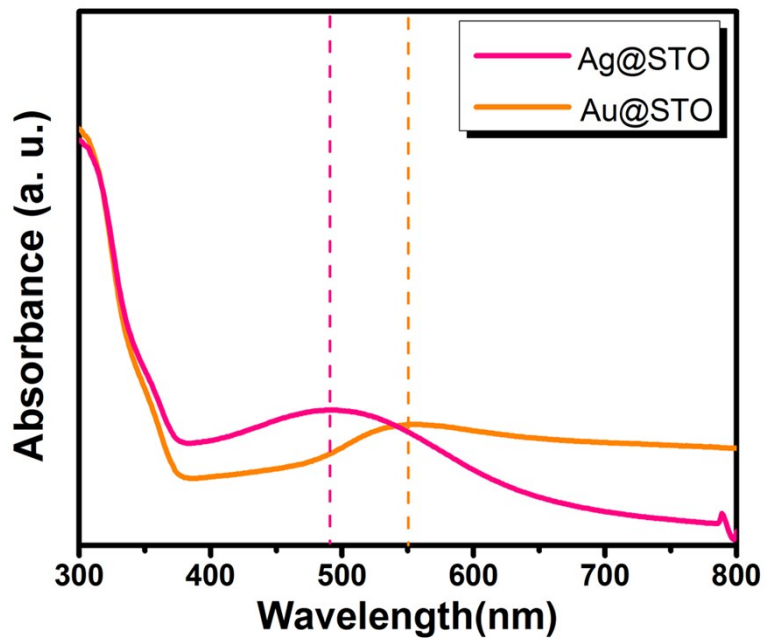


Figure S1. UV-visible absorption spectra of Ag@STO and Au@STO.

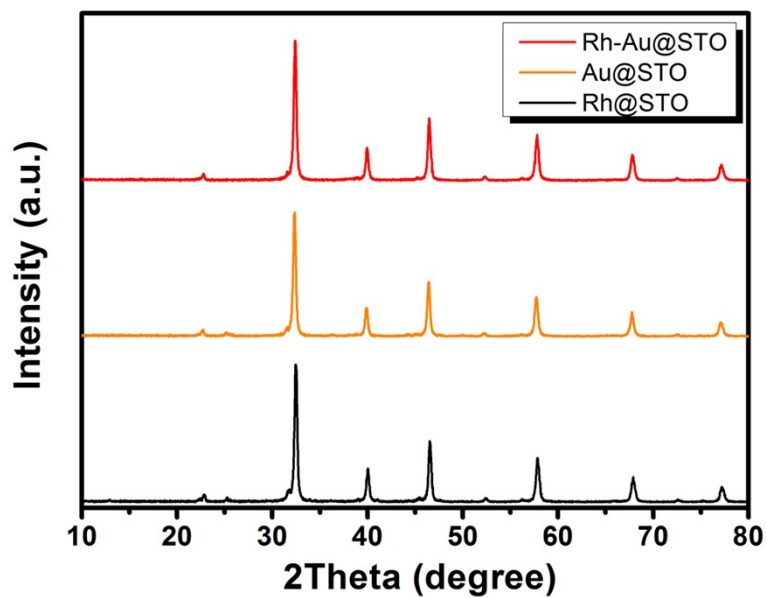


Figure S2. XRD patterns of Rh@STO, Au@STO, and Rh-Au@STO samples.

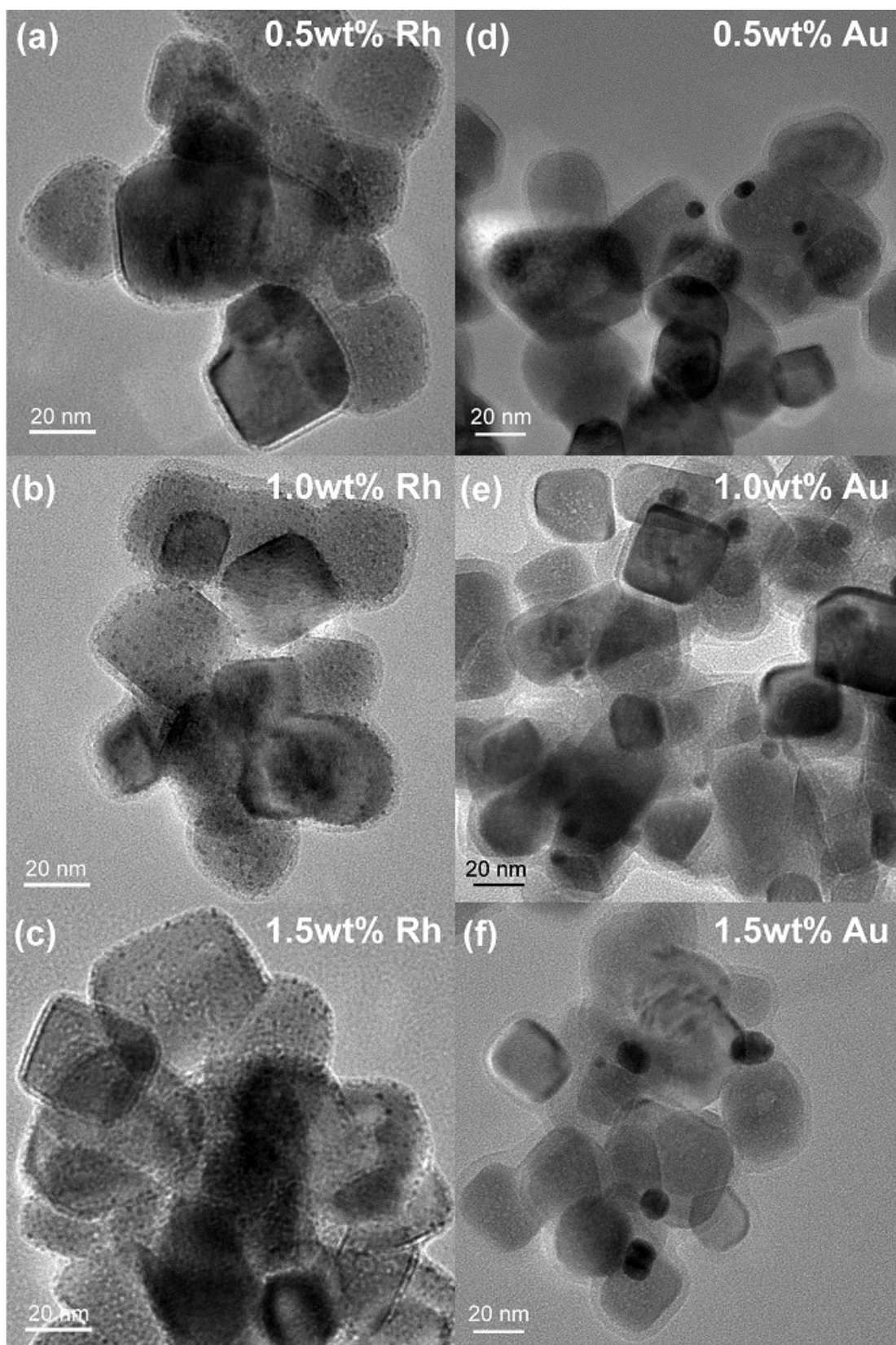


Figure S3. (a-c) TEM images of 0.5, 1.0 and 1.5wt% Rh loaded SrTiO₃ samples. (d-f) TEM images of 0.5, 1.0 and 1.5wt% Au loaded SrTiO₃ samples (mean sizes of Au nanoparticles in the three samples are estimated to be 9.6, 10.4, and 14.0 nm).

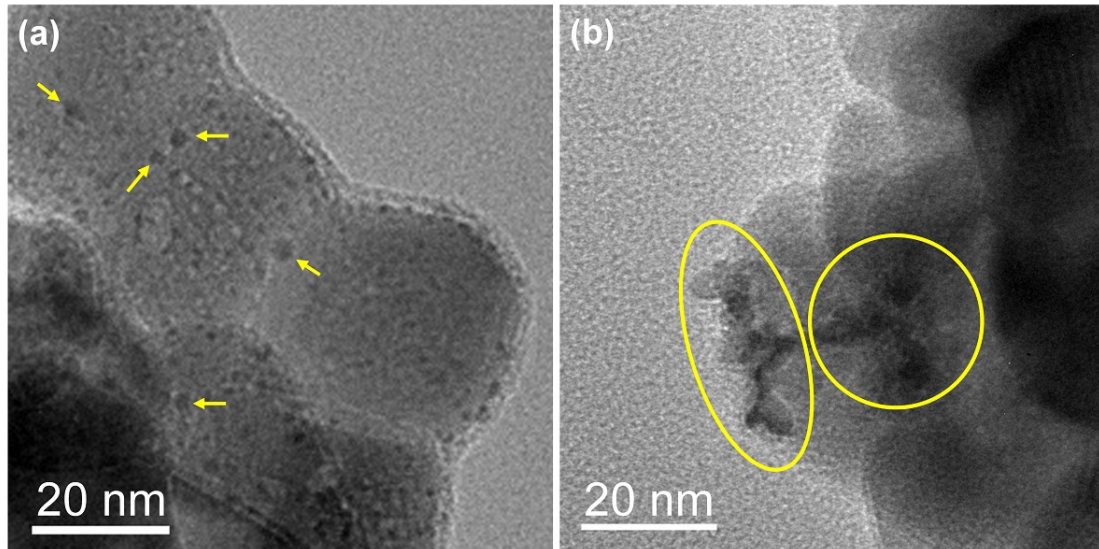


Figure S4. TEM images of Ru-loaded SrTiO₃ samples. (a) Ru nanoparticles prepared via impregnation, yellow arrows indicate well-dispersed bigger nanoparticles; (b) Ru nanoparticles synthesized by photodeposition, yellow circles show aggregations of Ru nanoparticles.

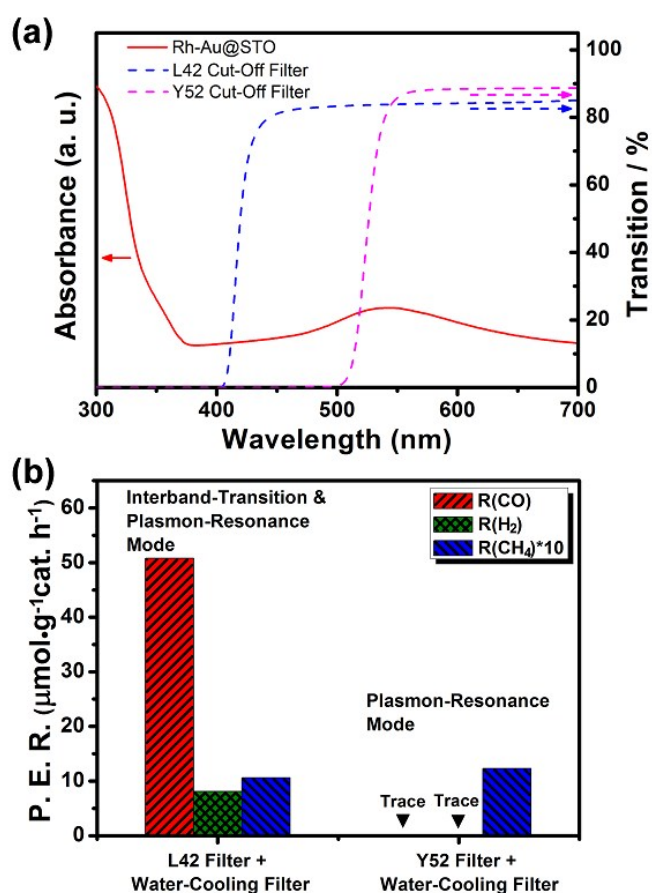


Figure S5. (a) UV-visible absorption spectrum of Rh-Au@STO sample and UV-visible transmission spectra of L42 and Y52 cut-off filters. (b) Photoactivities over Rh(PD)-Au@STO sample under different light-absorption modes; P. E. R., product evolution rate.

Note: The water-cooling filter can remove partial infrared light and prevent the damage of Y52 filter because of thermal effect. Compared to Fig. 3c, the obvious reduction of photoactivity over Rh(PD)-Au@STO in Fig. S5 can be reasonably explained as the decrease of both light intensity and thermal effect because of use of water-cooling filter.

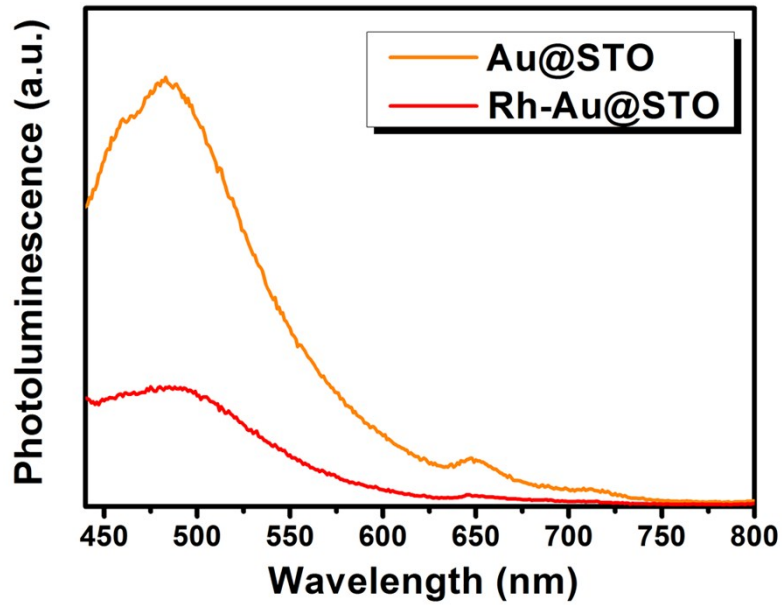


Figure S6. Photoluminescence (PL) spectra of Au@STO and Rh-Au@STO under light excitation with wavelength of 420 nm.

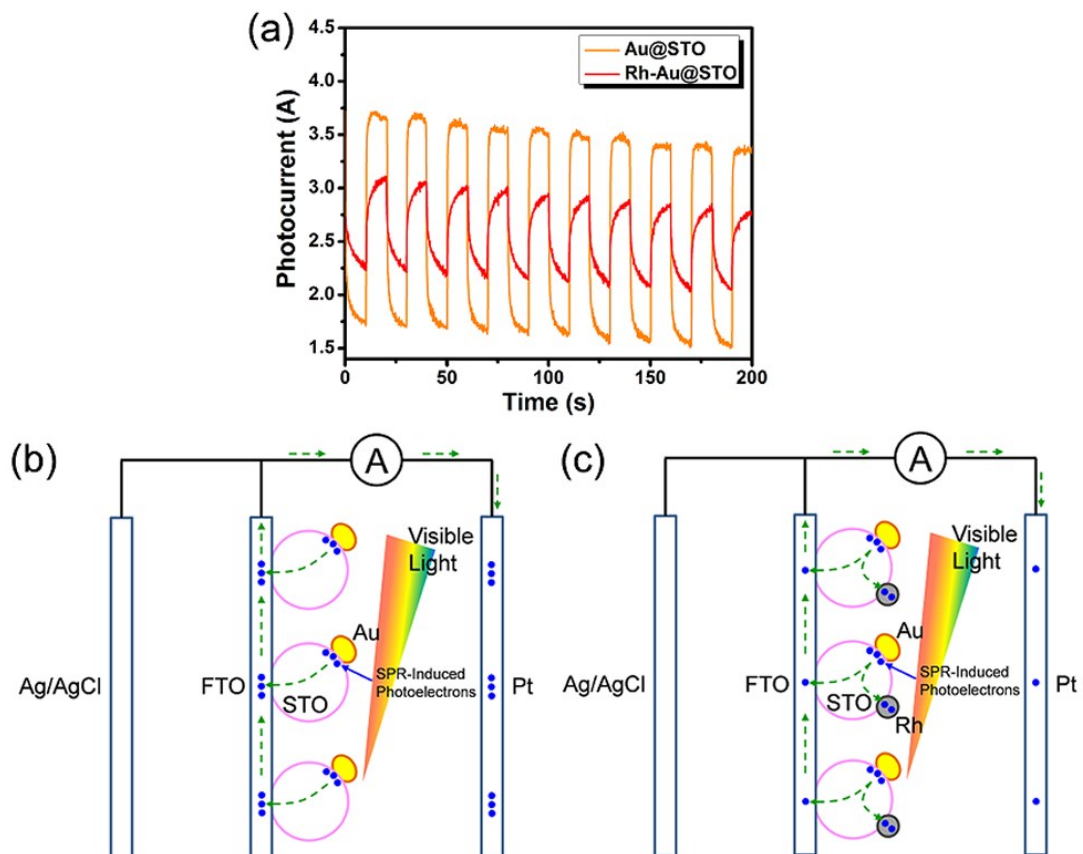


Figure S7. (a) Photocurrent - time ($I - t$) curves of Au@STO and Rh-Au@STO samples. (b, c) Schematic explanation for the photocurrent difference over Au@STO and Rh-Au@STO samples.

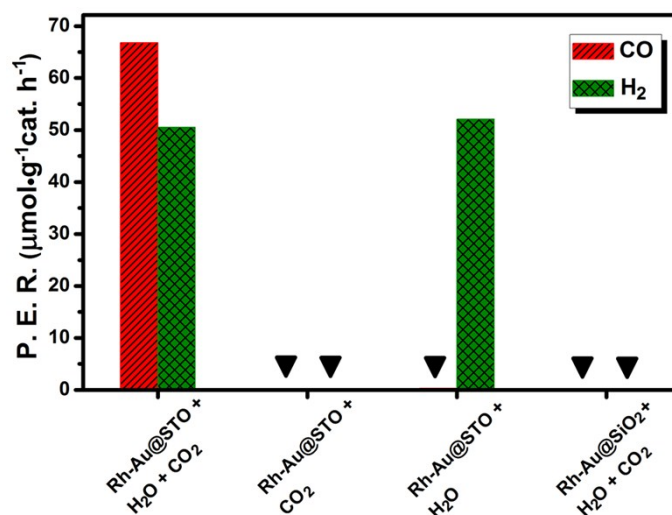


Figure S8. Control experiments for investigation of photoreduction of CO₂ and H₂O mixture. P. E. R., product evolution rate; inverted triangle means trace of evolution rate.

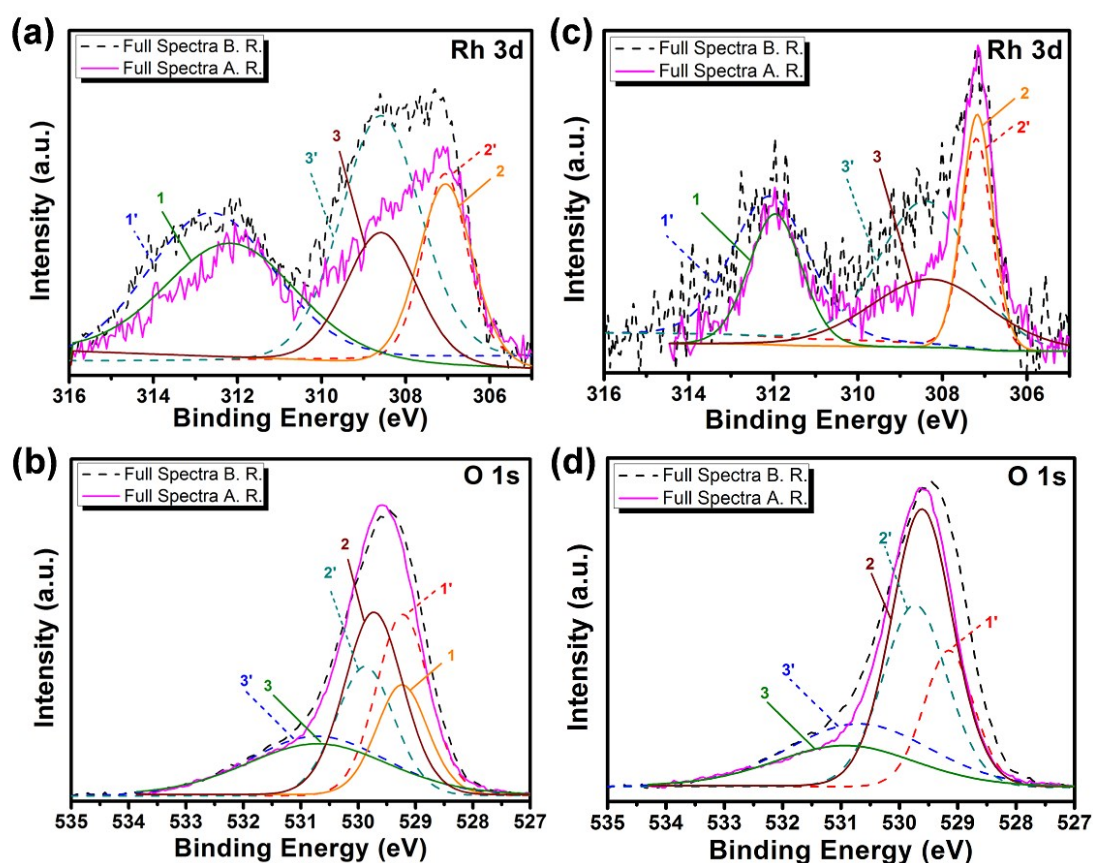


Figure S9. (a, b) Rh 3d and O 1s XPS spectra of Rh-Au@STO sample before reaction (B. R., dashed line) and after reaction (A. R., solid line). (c, d) Rh 3d and O 1s XPS spectra of Rh(PD)-Au@STO sample before reaction (B. R., dashed line) and after reaction (A. R., solid line). Curves 1' & 1, curves 2' & 2, and curves 3' & 3 in (a, c) correspond to deconvolution results of XPS spectra of Rh⁰ 3d_{3/2}, Rh⁰ 3d_{5/2}, and Rh³⁺ 3d_{5/2}, respectively; Curves 1' & 1, curves 2' & 2, and curves 3' & 3 in (b, d) associate with lattice O, adsorbed •O₂⁻, and -OH, respectively.

Table S2. Quantitative analyses of XPS spectra of O 1s and Rh 3d in Rh-Au@STO and Rh(PD)-Au@STO samples.

Peak Location (eV) (B. R. # / A. R. #)	Species	Proportion (B. R.) (%)	Proportion (A. R.) (%)
Rh-Au@STO Sample			
529.2 / 529.2	Lattice O	37.8	23.9
529.9 / 529.7	Adsorbed $\bullet\text{O}_2^-$	29.7	45.4
530.7 / 530.8	-OH	32.5	30.7
312.6 / 312.2	Rh ⁰ 3d _{3/2}	40.7	44.0
307.1 / 307.1	Rh ⁰ 3d _{5/2}	17.4	28.9
308.6 / 308.6	Rh ³⁺ 3d _{5/2}	41.9	27.1
Rh(PD)-Au@STO Sample			
529.2 / -	Lattice O	24.8	0
529.7 / 529.6	Adsorbed $\bullet\text{O}_2^-$	42.6	74.9
530.6 / 530.7	-OH	32.6	25.1
312.1 / 312.0	Rh ⁰ 3d _{3/2}	35.7	32.6
307.2 / 307.2	Rh ⁰ 3d _{5/2}	20.9	36.6
308.4 / 308.4	Rh ³⁺ 3d _{5/2}	43.4	30.8

B. R., before reaction; A. R., after reaction.

Discussion on the reductive and oxidative processes

The photogenerated electrons are mainly consumed through the reduction of CO₂ and H₂O into CO, H₂, and CH₄. The photooxidation process induced by positive-charged Au probably happened over the surface of SrTiO₃, since no oxidative product was detected. The XPS measurements just lend support to this supposition. The generated O₂ cannot be evolved, which generally can be attributed to that it stops at the status of adsorbed $\bullet\text{O}_2^-$ (a form of $-\text{Ti}-\text{O}-\text{O}-\text{Ti}-$). As shown in Table S2, surface lattice O and -OH were converted into adsorbed $\bullet\text{O}_2^-$ after photoreaction; in particular, the Rh(PD)-Au@STO sample with higher efficiency for syngas generation produced more amount of adsorbed $\bullet\text{O}_2^-$ (an increment of 32.3%) on its surface compared to the Rh-Au@STO sample (an enhancement of 15.7%). Therefore, the oxidative product in the present photoreaction of CO₂ reduction is surface adsorbed $\bullet\text{O}_2^-$.